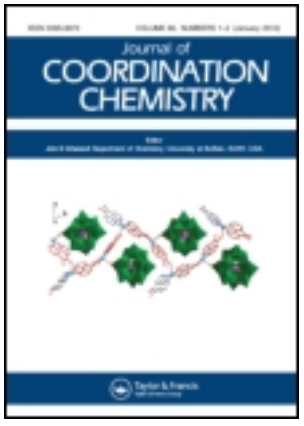

Journal of Coordination Chemistry
Publication details, including instructions for authors and subscription information:
http://www.tandfonline.com/loi/gcoo20

A copper(II) complex with 2-(2′-pyridyl)benzimidazole and l-arginine: synthesis, structure, antibacterial activities, and DNA interaction

Zhi Bin Ou [a], Yu Hao Lu [a], Yan Mei Lu [a], Shi Chen [a], Ya Hong Xiong [a], Xiao Hua Zhou [a], Zong Wan Mao [b c] & Xue Yi Le [a b c]

[a] Laboratory of Bioinorganic Chemistry, South China Agricultural University, Guangzhou, P.R. China

[b] Institute of Biomaterials, South China Agricultural University, Guangzhou, P.R. China

[c] School of Chemistry and Chemical Engineering, Zhongshan University, Guangzhou, P.R. China

Accepted author version posted online: 29 Apr 2013.Published online: 30 May 2013.

To cite this article: Zhi Bin Ou, Yu Hao Lu, Yan Mei Lu, Shi Chen, Ya Hong Xiong, Xiao Hua Zhou, Zong Wan Mao & Xue Yi Le (2013) A copper(II) complex with 2-(2′-pyridyl)benzimidazole and l-arginine: synthesis, structure, antibacterial activities, and DNA interaction, Journal of Coordination Chemistry, 66:12, 2152-2165, DOI: 10.1080/00958972.2013.800195

To link to this article: http://dx.doi.org/10.1080/00958972.2013.800195

Journal of Coordination Chemistry, 2013
Vol. 66, No. 12, 2152–2165, http://dx.doi.org/10.1080/00958972.2013.800195

A copper(II) complex with 2-(2′-pyridyl)benzimidazole and L-arginine: synthesis, structure, antibacterial activities, and DNA interaction

ZHI BIN OU†, YU HAO LU†, YAN MEI LU†, SHI CHEN†, YA HONG XIONG, XIAO HUA ZHOU†, ZONG WAN MAO‡,§ and XUE YI LE*†,‡

†Laboratory of Bioinorganic Chemistry, South China Agricultural University, Guangzhou, P.R. China
‡Institute of Biomaterials, South China Agricultural University, Guangzhou, P.R. China
§School of Chemistry and Chemical Engineering, Zhongshan University, Guangzhou P.R. China

(*Received 23 February 2012; in final form 27 February 2013*)

A Cu(II) complex with 2-(2′-pyridyl)benzimidazole and L-arginine has been synthesized and investigated by elemental analysis, molar conductivity, IR, UV/vis, and X-ray diffraction. The complex crystallizes in the triclinic space group *P*1 with six molecules in a unit cell of dimensions $a = 10.6397(5)$ Å, $b = 19.2178(8)$ Å, $c = 20.0387(9)$ Å, $\alpha = 75.3670(10)°$, $\beta = 79.4670(10)°$, $\gamma = 87.4470(10)°$, $V = 3897.6(3)$ Å^3, $R_1 = 0.0408$, and w$R_2 = 0.0502$. The complex contains six crystallographically independent complexes, **Cu1**, **Cu2**, **Cu3**, **Cu4**, **Cu5**, and **Cu6**, which have a distorted square-pyramidal geometry. The complex was screened for its *in vitro* antibacterial activities against two Gram-positive (*Bacillus subtilis* and *Staphylococcus aureus*) and two Gram-negative (*Escherichia coli* and *Salmonella*) micro-organisms. The complex exhibited good antibacterial activities against the micro-organisms compared with HPB and $Cu(ClO_4)_2$. Interaction of the complex with DNA was studied by electronic absorption spectroscopy, fluorescence spectroscopy, circular dichroic spectroscopy, viscosity measurements, and agarose gel electrophoresis. Results suggest that the complex could bind to CT-DNA via partial intercalation, and cleave the plasmid DNA with involvement of hydroxyl radicals, and probably singlet oxygen-like copper-oxo species in the presence of ascorbate.

Keywords: 2-(2′-Pyridyl)benzimidazole; L-Arginine; Copper(II) complex; Crystal structure; Antibacterial activities; DNA

1. Introduction

Transition metal complexes with L-α amino acids and N-heterocyclic ligands such as 1,10-phenanthroline and 2,2′-bipyridine have drawn wide attention for their potential applications as probes of DNA structure, chemical nucleases, SOD mimics, and chemtherapeutic agents [1–6]. Among N-heterocyclic ligands are benzimidazole and its 2-substituted derivatives which display a wide range of biological activities including antibacterial, antifungal, antiamobeic, antimicrobial, antiparasitic, and antitumor [7–13]. Recent studies showed that

*Corresponding author. Email: lexy@scau.edu.cn

the combination of pharmaceutical agents with metal ions can improve their biological activities and decrease their toxicity [12–14]. Incorporation of biological ligands such as L-α-amino acids in the complex systems with the drug molecules and metal ions may increase biocompatibilities and antibacterial activities [15].

Copper is an important biometal with role in proteins and its potential synergetic activity with drugs [16]. Copper(II) complexes with drugs have potential antitumor, antioxidant, antibacterial, and antifungal activity [17]. Hence, investigation of copper(II) complexes of benzimidazole and its 2-substituted derivatives with L-α amino acids is of importance in the search for more effective drugs.

Recently, we reported synthesis, structure, DNA binding properties and biological activity of a series of new copper(II) complexes with 2-substituted benzimidazole derivatives and L-α amino acids, and found that the complexes have good DNA binding properties and antibacterial activities [6, 15, 18]. As continuation of our work, herein, we present syntheses, structure, antibacterial activities, and DNA interaction of a copper(II) complex with 2-(2′-pyridyl)benzimidazole and L-arginine. The results should be valuable in understanding the interaction mode of the complex with DNA as well as laying a foundation for design of novel antibacterial reagents.

2. Experimental

2.1. *Materials and measurement*

2-(2′-Pyridyl)benzimidazole was prepared according to the method described in the literature [19]. Calf thymus DNA (CT-DNA), ascorbate, and agarose (molecular biology grade) and ethidium bromide (EB) (molecular biology grade) were obtained from the Sigma Company. Plasmid pBR322 DNA was provided by Huamei Chemical Company (Beijing, China). Luria Broth was obtained from Guangdong Huankai Microbial Sci. & Tech. Co. LTD (China). Other chemicals and reagents were commercially available and of reagent grade. UV absorbance at 260 and 280 nm of CT-DNA in the tris(hydroxylmethyl)methane-HCl(Tris–HCl) buffer solution (5 mM L^{-1} Tris–HCl, 50 mM L^{-1} NaCl, pH = 7.2) gave a ratio of $\sim 1.9 (A_{260\,nm}/A_{280\,nm})$, indicating that the DNA was sufficiently free of protein [20]. The DNA concentration per nucleotide was determined by electronic absorption spectroscopy using the molar absorption coefficient ($LM^{-1}\,cm^{-1}$) at 260 nm, taking the molar absorption coefficient (ε_{260}) of CT-DNA as $6600\,M^{-1}\,cm^{-1}$ [21]. The Gram-negative (*Escherichia coli* and *Salmonella*) and Gram-positive (*Bacillus subtilis* and *Staphylococcus aureus*) micro-organisms were provided by Guangdong Key Laboratory of Plant Molecular Breeding, South China Agricultural University. Stock solution of CT-DNA was stored at 277 K and used after no more than 4 days. Double distilled water was used throughout.

The elemental analysis was done using a Vario EL elemental analyzer. The infrared spectrum was recorded from 4000 to 400 cm^{-1} on a Nicolet ACATAR 360 FTIR spectrometer with samples as KBr pellets. The molar conductivity at room temperature was measured in $1 \times 10^{-3}\,ML^{-1}$ methanol solution using a DSS-12A digital molar conductometer. The electronic and fluorescence spectra were recorded on a Amersham Pharmacia Biotech UV–vis 4000 spectrophotometer and a Hitachi RF-4500 spectrophotometer, respectively, at room temperature.

2.2. *Synthesis of the complex*

The complex was prepared by a general synthetic method in which a mixture of 2-(2′-pyridyl)benzimidazole (0.5 mM) and $Cu(ClO_4)_2$ (0.5 mM) in 20 mL ethanol was added dropwise to an aqueous solution (5 mL) of L-arginine (0.5 mM) and NaOH (0.5 mM) with stirring for about 20 min. The resulting solution was left to evaporate slowly at room temperature. After 40 days, light green crystals were obtained. Yield: 73%. Anal. Calcd (%) for $C_{18}H_{27}Cl_2CuN_7O_{12}$ (Mr = 667.91): C, 32.37; H, 4.07; N, 14.68. Found (%): C, 32.20; H, 4.15; N, 14.74.

2.3. *X-ray structural determination of the complex*

A well-shaped crystal of the complex with approximate dimensions $0.44 \times 0.39 \times 0.36\,mm^3$ was mounted on a Bruker Smart 1 K CCD diffractometer with graphite monochromated Mo-$K\alpha$ radiation at $\lambda = 0.71073$ Å. The SMART program was applied to search for diffraction peaks to determine cell parameters, and the collected data were reduced with the SAINT + program [22]. Empirical absorption corrections were carried out using the Siemens Area Detector ABSorption program [23]. The structure was solved by direct and Fourier methods and refined by full-matrix least squares on F^2 with positional and anisotropic thermal parameters. Hydrogens were placed in calculated positions. Atomic scattering factors and anamolous dispersion corrections were taken from International Tables for X-ray Crystallography [24]. All calculations were performed on a PC with the Siemens SHELXTL software packages [25]. The crystal data, some experimental details of data collection and refinement for the complex are listed in table 1. Selected bond lengths and angles are collected in tables 2 and 3, respectively. Crystallographic data for the complex have been deposited in the Cambridge Crystallographic Data Center (12 Union Road, Cambridge, CB2 1EZ, UK) as supplementary publications and are available on request quoting no. CCDC-826626.

2.4. *Antibacterial activities*

The antibacterial activities of the compounds (the complex, copper(II) perchlorate, and HPB), were investigated against two gram-negative (*E. coli* and *Salmonella*) and two gram-positive (*B. subtilis* and *S. aureus*) micro-organisms.

A standard volume (10 mL) of Luria broth medium (1% peptone, 0.5% NaCl, and 0.5% beef, pH = 7.4 ± 0.2) used to support the growth of the micro-organisms was added to several labeled sterile identical assay tubes. The minimal inhibitory concentrations (MICs) of the complex for the four micro-organisms were determined using a series of two-fold serial dilutions. Dilutions for $Cu(ClO_4)_2$ and HPB were prepared and a control tube containing no test compound was also included. Bacterial growth was monitored after 24 h. If a certain concentration of a compound inhibited bacterial growth, half the concentration of the compound was tested. This procedure was continuously carried out to a concentration at which bacteria can grow normally. The lowest concentration that inhibited bacterial growth was called as the MIC value. All the experiment and culture media were sterile.

Table 1. Crystal data, experimental details of data collection and refinement for $[Cu(HPB)(L\text{-}Arg)(H_2O)](ClO_4)_2$.

Empirical formula	$C_{18}H_{27}Cl_2Cu_1N_7O_{12}$
Formula weight	667.91
Crystal system	Triclinic
Temperature (K)	110(2)
λ (Mo Kα) (Å)	0.71073
Space group	$P1$
Unit cell dimensions (Å, °)	$a = 10.6397(5)$, $\alpha = 75.3670(10)$ $b = 19.2178(8)$, $\beta = 79.4670(10)$ $c = 20.0387(9)$, $\gamma = 87.4470(10)$
V (Å^{-3})	3897.6(3)
Z	6
D_{calc} (g cm^{-3})	1.707
μ (Mo Ka) (mm^{-1})	1.122
F (000)	2058
Crystal size (mm^3)	$0.44 \times 0.39 \times 0.36$
θ range for data collection (°)	1.10–26.00
Index ranges	$-13 \leqslant h \leqslant 13$, $-23 \leqslant k \leqslant 23$, $-24 \leqslant l \leqslant 24$
Reflections collected	30,123
Independent reflections	26,949
R_{int}	0.0191
Absorption correction	Semi-empirical from equivalents
Max. and min. transmission	0.6882 and 0.6381
Refinement method	Full-matrix least-squares on F^2
Data/restraints/parameters	26,949/78/2258
Absolute structure parameter	−0.011(8)
Goodness-of-fit on F^2	1.024
Final R indices [$I > 2\sigma(I)$]	$R_1 = 0.0408$, $wR_2 = 0.0977$
R indices (all data)	$R_1 = 0.0562$, $wR_2 = 0.1095$
Largest difference peak and hole (e Å^{-3})	0.903 and −0.395

Table 2. Selected bond lengths (Å) for $[Cu(HPB)(L\text{-}Arg)(H_2O)](ClO_4)_2$ with e.s.d.s in parentheses.

	Cu–Npy	Cu–Nbzi	Cu–NArg	Cu–OArg	Cu–Owater
Cu1	2.020(5)	1.989(4)	1.970(4)	1.940(4)	2.340(4)
Cu2	2.028(4)	2.001(4)	1.987(4)	1.929(4)	2.308(4)
Cu3	2.027(4)	1.992(4)	1.984(4)	1.954(3)	2.345(4)
Cu4	2.015(4)	1.986(4)	2.001(4)	1.957(3)	2.307(3)
Cu5	2.032(4)	2.004(4)	1.973(4)	1.949(4)	2.284(4)
Cu6	2.020(4)	1.977(4)	1.998(4)	1.959(3)	2.356(3)

2.5. *DNA-binding experiments*

2.5.1. The electronic spectra. Absorption titration measurements were done by varying the concentration of CT-DNA (0–12.99×10^{-5} M L^{-1}), keeping the copper complex concentration constant (1.0×10^{-4} M L^{-1}) in the buffer solution (5×10^{-3} M L^{-1} Tris–HCl/ 5×10^{-2} M L^{-1} NaCl buffer, pH = 7.2). Samples were kept for equilibrium before recording each spectrum.

2.5.2. Fluorescence spectra. Fluorescence spectra were recorded at room temperature with excitation at 550 nm and emission at 650 nm. 5.5×10^{-5} M L^{-1} CT-DNA was pretreated with 4.8×10^{-5} M L^{-1} EB for 30 min. The complex (0–5.30×10^{-5} M L^{-1}) was then added to the mixture and the effect on emission intensity was measured.

2.5.3. Viscosity measurement. Viscosity measurement of 2×10^{-4} M L^{-1} CT-DNA in Tris-HCl/NaCl buffer was performed using an Ubbelodhe viscometer thermostated at 29 (±0.1) °C in a constant temperature bath. Data are presented as $(\eta/\eta_0)^{1/3}$ *versus* binding ratio [Complex]/[DNA], where η and η_0 indicate the specific viscosity of DNA solutions in the presence and absence of complex, respectively. The relative specific viscosity was calculated according to the relation $\eta = (t - t_o)/t_o$, where t is the flow time of DNA solution in the presence or absence of complex and t_o is the flow time of the buffer alone [26]. Flow time was measured with a digital stopwatch; each sample was measured three times and an average flow time was calculated.

2.6. *DNA cleavage experiments*

The DNA cleavage properties of the complex were studied by agarose gel electrophoresis. The gel electrophoresis experiments were performed by incubation at room temperature as follows: 200 ng pBR322 DNA and 25 μM L^{-1} tested compounds ($Cu(ClO_4)_2$, HPB, and the complex) in the presence of ascorbate (1.25 mM L^{-1}) in Tris–HCl buffer (pH = 7.2) to yield a total volume of 20 μL for 5 min. The samples were then electrophoresed at 100 V and 28 °C for 40 min on 0.8% agarose gel in TBE buffer (4.5×10^{-2} M L^{-1} Tris $+ 4.5 \times 10^{-2}$ M L^{-1} $H_3BO_3 + 10^{-3}$ M L^{-1} EDTA, pH = 8.3). The gel bands were stained using 4 and 5 μL Gold View and photographed under ultraviolet light. The mechanistic studies for DNA cleavage were performed using 4 μM L^{-1} different additives, DMSO, and NaN_3, before addition of the complex according to the above procedures.

3. Results and discussion

3.1. *General aspects*

Elemental analysis data of the complex are in agreement with $C_{18}H_{27}Cl_2CuN_7O_{12}$. The molar conductivity for the complex in methanol is 189.2 S cm^2 M^{-1}, indicating that the complex should be a 1 : 2 electrolyte [27], as expected by single-crystal X-ray crystallography.

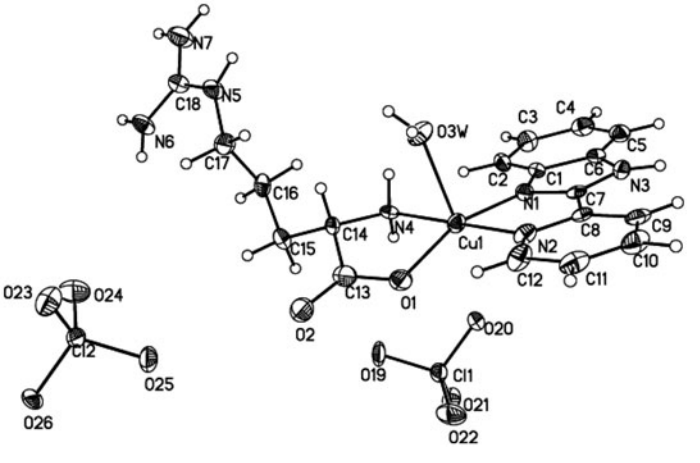

Figure 1. ORTEP drawing of [Cu(HPB)(L-Arg)(H_2O)](ClO_4)$_2$.

Table 3. Selected bond angles (°) for [Cu(HPB)(L-Arg)(H_2O)](ClO_4)$_2$ with e.s.d.s in parentheses.

	OArg–Cu–NArg	OArg–Cu–Nbzi	NArg–Cu–Nbzi	OArg–Cu–Npy	NArg–Cu–Npy	Nbzi–Cu–Npy	OArg–Cu–Owater	NArg–Cu–Owater	Nbzi–Cu–Owater	Npy–Cu–Owater
Cu1	84.19(16)	161.28(16)	102.31(17)	92.51(17)	175.17(19)	81.91(18)	95.02(15)	86.39(15)	102.84(16)	90.39(15)
Cu2	85.30(15)	161.34(16)	101.02(17)	91.53(17)	176.14(18)	81.34(18)	95.31(15)	91.07(15)	102.04(16)	91.42(16)
Cu3	84.44(16)	164.43(16)	100.33(17)	92.61(16)	175.91(17)	81.80(18)	94.58(14)	92.81(15)	99.94(15)	90.24(15)
Cu4	84.09(15)	163.30(15)	100.06(17)	95.50(16)	175.25(18)	81.68(18)	94.51(14)	87.93(15)	101.77(16)	87.39(15)
Cu5	84.43(16)	170.19(16)	98.39(17)	95.24(16)	177.50(17)	81.53(18)	94.04(14)	93.53(15)	95.15(15)	88.97(15)
Cu6	84.11(15)	164.44(15)	99.86(16)	94.84(16)	176.15(17)	82.13(17)	94.74(14)	86.52(15)	100.49(15)	89.88(15)

3.2. *Crystal structure*

The local coordination structure of the complex is shown in figure 1. The structure analysis indicates that the complex crystallizes in the triclinic space group *P*1 with six molecules in the unit cell, and consists of $[Cu(HPB)(L\text{-}Arg)(H_2O)]^{2+}$, slightly distorted perchlorates, and crystallization waters packed with each other by electrostatic bonding, and hydrogen-bonding interactions (table 3). The crystal of the complex contains six crystallographically independent complexes: **Cu1**, **Cu2**, **Cu3**, **Cu4**, **Cu5**, and **Cu6** in the unit cell. All the complexes have a distorted square-pyramidal geometry with each central Cu (II) coordinating two nitrogens of HPB and the amino nitrogen, and one carboxylate oxygen of the zwitterionic L-arginine in the equatorial positions (Cu–Npy = 2.015(4)–2.032(4) Å, Cu–Nbzi = 1.986(4)–2.004(4) Å, Cu–NArg = 1.970(4)–2.001(4) Å, and Cu–OArg = 1.929 (4)–1.957(3) Å, and a water at the axial position (Cu–Owater = 2.284(4)–2.356(3) Å, indicating that perchlorates were not coordinated, in agreement with the result obtained by molar conductivity. Bond angles between adjacent equatorial positions around the copper (II) ions are 81.34(18)–102.31(17)°, and ones between the equatorial positions and the axial positions are 86.39(15)–102.84(16)°, showing the angle variability in the five-coordinate Cu(II) complexes. The carboxyl of the amino acid coordinates via one oxygen as a unidentate coordination group, and electron delocalization is observed in the carboxyl group, in which the bond distances (1.276(6)–1.286(8) Å) between the coordinated oxygens and carbon are slightly longer than those (1.232(6)–1.246(6) Å) between uncoordinated oxygen and carbon as expected. The aforementioned bond lengths and angles are comparable to related data observed for $[Cu(PBT)(L\text{-}Ala)(H_2O)]ClO_4$ and $[Cu(HPB)(L\text{-}Ala)(ClO_4)(H_2O)]_2{\cdot}H_2O$ [6,28]. In addition, if the difference of the corresponding bond lengths and angles are omitted, **Cu1**, **Cu3**, and **Cu5** are essentially the same (as are **Cu2**, **Cu4**, and **Cu6**), and the enantiomers of **Cu2**, **Cu4** and, **Cu6**.

Table 4. Selected hydrogen-bonding parameters in the crystal of the complex.

D-H···A	*D*–H (Å)	H…A (Å)	*D*…A (Å)	*D*–H…A (°)
N(3)–H(3B)···O(58)	0.88	1.98	2.825(6)	161.3
N(4)–H(4A)···O(45) #1	0.92	2.16	3.072(6)	172.8
N(5)–H(5A)···O(17) #1	0.88	2.09	2.909(5)	154.6
N(6)–H(6A)···O(35) #2	0.88	2.19	3.049(6)	165.2
N(6)–H(6B)···O(28) #2	0.88	2.16	2.992(5)	157.3
N(7)–H(7A)···O(17) #1	0.88	2.36	3.066(6)	137.9
N(7)–H(7B)···O(54) #2	0.88	2.19	2.934(6)	142.7
O(3 W)–H(3A)···O(50)	0.89(3)	1.989(17)	2.858(10)	163(4)
O(3 W)–H(3C)···O(69 W) #3	0.890(10)	1.858(12)	2.730(6)	166(3)
O(71 W)–H(71D)···O(2)	0.91	2.40	2.938(5)	118.0
O7(1 W)–H(71E)···O(1)	0.90	2.35	3.157(5)	148.3
O(72 W)–H(72D)···O(2)	0.99(6)	1.69(7)	2.666(6)	167(6)
N(17)–H(17C)···O(20)	0.88	2.00	2.840(6)	160.1
N(25)–H(25A)···O(22)	0.92	2.19	3.104(6)	173.0
N(26)–H(26A)···O(2)	0.88	2.27	3.150(6)	176.1
N(28)–H(28B)···O(23) #4	0.88	2.09	2.962(5)	172.4
N(32)–H(32B)…O(24) #5	0.92	2.19	3.081(5)	163.7
N(33)–H(33C)…O(25) #5	0.88	2.38	3.039(5)	131.9
N(34)–H(34D)…O(19) #6	0.88	2.48	3.141(6)	132.1

Symmetry transformations used to generate equivalent atoms: #1 $x, y+1, z-1$; #2 $x+1, y, z-1$; #3 $x, y, z-1$; #4 $x+1, y, z$; #5 $x, y, z+1$; #6 $x-1, y, z+1$.

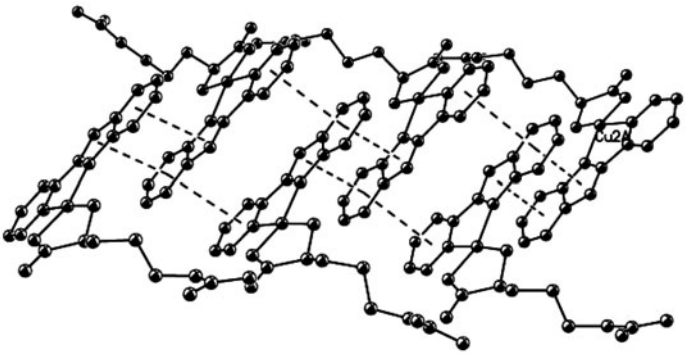

Figure 2. Intermolecular aromatic-ring stacking diagram in the crystals for [Cu(HPB)(L-Arg)(H_2O)](ClO_4)$_2$.

In crystals of the complex, independent molecules are packed with hydrogen bonding interactions (table 4) and intermolecular aromatic ring stacking interactions (figure 2), in which the average distance between benzene ring centroid and imidazole ring centroid is 3.60713 Å, and that between benzene ring centroid and pyridine ring centroid is 3.58013 Å.

3.3. *Infrared absorption spectrum*

In the IR spectrum, strong bands at 3422, 3270, and 2921 cm^{-1} can be ascribed to the stretching vibrations ν_{-O-H}, $\nu^{as}_{-NH_2}$, and $\nu^{s}_{-NH_2}$, respectively. The absence of a band at 1750–1700 cm^{-1} suggests coordination of COO^- of L-Arg. Bands at 1653 and 1396 cm^{-1} can be attributed, respectively, to antisymmetric and symmetric stretching vibrations ($\nu^{as}_{-COO^-}$ and $\nu^{s}_{-COO^-}$) of coordinated carboxylate. The unidentate coordination of carboxylate was characterized by $\Delta\nu_{COO-}$ ($\nu^{as}_{-COO^-} - \nu^{s}_{-COO^-} > 200\ cm^{-1}$) [29, 30]. Thus, it may be concluded that L-Arg is coordinated to the metal ion as a N,O-bidentate ligand, in agreement with the result obtained by the single-crystal X-ray diffraction. The band at 1486 cm^{-1} is assigned to the stretching vibration of the C=N of HPB and confirms its coordination [31]. Alternatively, this band could be assigned to the deformation mode NH of the N–H group belonging to the amino acid moiety [32].

3.4. *Electronic absorption spectrum*

The electronic absorption spectrum of the complex in methanol presents three important absorption bands. The two bands at 241 nm ($\varepsilon = 13{,}200\ L\,M^{-1}\,cm^{-1}$) and 325 nm ($\varepsilon = 13{,}893\ L\,M^{-1}\,cm^{-1}$) can be ascribed to $\pi \rightarrow \pi^*$ transitions of coordinated HPB, and the broad and weak absorption at 623 nm ($\varepsilon = 76\ L\,M^{-1}\,cm^{-1}$) to the $d \rightarrow d$ transition of Cu(II), similar to the related 2-substituted benzimidazole derivatives – Cu(II)-amino acid complexes [4, 6]. The results indicate that Cu(II) in the solution has a square pyramidal coordination geometry [33].

3.5. *Antibacterial activity*

The efficiencies of [Cu(HPB)(L-Arg)(H_2O)](ClO_4)$_2$, HPB, and Cu(ClO_4)$_2$ have been tested with a series of two-fold serial dilutions against two Gram-negative (*E. coli* and

Table 5. MIC ($\mu g\,mL^{-1}$) of $Cu(ClO_4)_2$, HPB and $[Cu(HPB)(L\text{-}Arg)(H_2O)](ClO_4)_2$ for the assayed bacteria.

Compound	*B. subtilis*, G+	*S. aureus*, G+	*Salmonella*, G−	*E. coli*, G−
$Cu(ClO_4)_2$	320	320	256	256
HPB	256	200	256	160
$[Cu(HPB)(L\text{-}Arg)(H_2O)](ClO_4)_2$	80	80	80	64

Salmonella) and two Gram-positive (*B. subtilis* and *S. aureus*) micro-organisms. The minimum inhibitory concentrations (MICs) expressed in $\mu g\,mL^{-1}$ are summarized in table 5. MICs of $[Cu(HPB)(L\text{-}Arg)(H_2O)](ClO_4)_2$ against the bacteria are lower than those of copper(II) perchlorate salt and HPB. Generally, coordination can reduce the polarity of Cu(II) because of partial sharing with the aromatic amine by π-electron delocalization within the chelate aromatic ring, increasing lipophilic character allowing metal ion to get across the semipermeable membrane barrier and interfere in normal cell processes [34].

3.6. *DNA-binding effect*

The interaction of metal complexes with DNA is important for development of effective chemotherapeutic agents. DNA-binding properties of the complex have been studied by electronic absorption spectroscopy, fluorescence spectroscopy, and viscosity measurements.

3.6.1. Electronic absorption spectroscopy. Electronic absorption spectroscopy is an effective tool to determine the binding modes of metal complexes with DNA. Spectra of the complex from 230 to 450 nm in the absence and presence of CT-DNA are shown in figure 3, in which the band at 330 nm can be attributed to the $\pi\rightarrow\pi^*$ transition of coordinated HPB.

As the DNA concentration increased, the absorption peak intensity of the complex decreased remarkably, indicating that the complex may bond to CT-DNA by an intercalative mode [35, 36].

In order to further illustrate the binding strength of the complex, the intrinsic binding constant K_b for the interaction of the complex with CT-DNA was calculated using the absorption at 330 nm by adopting the following equation:

$$[DNA]/(\varepsilon_a - \varepsilon_f) = [DNA]/(\varepsilon_b - \varepsilon_f) + 1/K_b(\varepsilon_b - \varepsilon_f)$$

where ε_a, ε_f, and ε_b correspond to (A_{obsd}/[Cu]), the extinction coefficient for the free copper (II) complex and extinction coefficient for the copper(II) complex in the fully bound form, respectively. By plotting $[DNA]/(\varepsilon_a - \varepsilon_f)$ versus [DNA], K_b is the ratio of the slope to the intercept of the linear plot [37]. From the inset in figure 3, obtained by using the absorptions at 313 nm, the K_b value for the complex was $2.478 \times 10^5\,L\,M^{-1}$, comparable to one observed for the corresponding complex with L-methioninate [17], but lower than that of classical intercalator EB (K_b, $1.4 \times 10^6\,L\,M^{-1}$ in $25\,m\,M\,L^{-1}$ Tris–HCl/$40\,m\,M\,L^{-1}$ NaCl buffer, pH 7.9) [38]. The result suggests that the copper complex has a weaker binding of DNA compared with the classical intercalator [39].

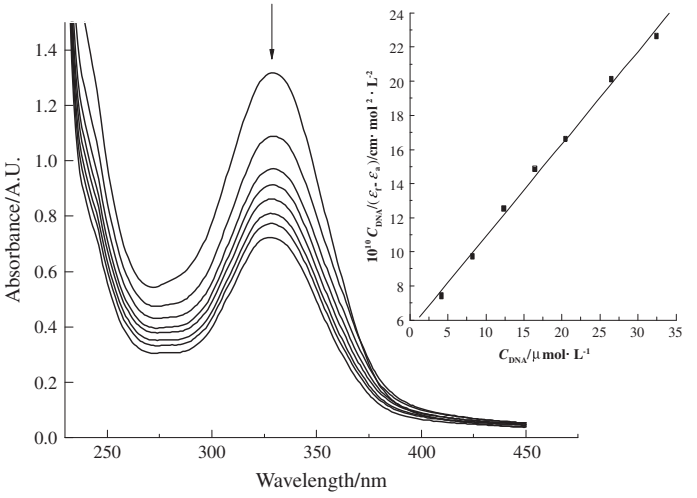

Figure 3. Absorption spectra of the complex in the absence of CT-DNA (1) and in the presence of increasing amounts of CT-DNA (2–9), [complex] = 1.0×10^{-4} M L^{-1}, [DNA]/(10^{-5} M L^{-1}): 0, 2.439, 4.800, 9.302, 13.53, 17.52, 21.28, 24.83, 28.19. Arrow shows the absorbance changes upon increasing CT-DNA concentrations.

3.6.2. Fluorescence spectroscopy. The emission intensity of EB can be used as a spectral probe as EB exhibits no apparent emission intensity in buffer solution because of solvent quenching and shows an enhancement of the emission intensity when intercalatively bound to CT-DNA [40]. Therefore, the extent of fluorescence quenching for EB bound to CT-DNA can be used to determine the extent of binding between the complex and CT-DNA, in which the complex did not show any fluorescence at room temperature in solution or in the presence of CT-DNA. In this study, the emission spectra of EB bound to CT-DNA in the absence and presence of the complex with different concentrations are given in figure 4.

The results show that the fluorescence intensity of CT-DNA-EB system decreased gradually with addition of the complex, indicating that the complex can replace EB from DNA, and a complex-CT-DNA system was formed. The linear Stern-Volmer quenching constant K_{sq} can be calculated according to the following Stern-Volmer equation [41]:

$$I_0/I = 1 + K_{sq}r$$

where I_0 and I correspond to fluorescence intensities in the absence and presence of the complex, respectively, and r is the concentration ratio of the complex to CT-DNA. The quenching constant K_{sq}, dependent on the ratio of the bound concentration of EB to the concentration of CT-DNA, can be obtained from the linear regression of I_0/I with r. As can be seen from the inset in figure 4, the quenching of EB bound to CT-DNA by the complex is in agreement with the linear Stern-Volmer equation, indicating that CT-DNA is influenced by the complex in the intercalation binding mode [42]. The obtained K_{sq} value for the complex is 0.09552, indicating that the complex has weaker intercalation to CT-DNA, consistent with the result obtained from electronic absorption spectra.

3.6.3. Viscosity measurement. Optical photophysical probes generally provide necessary but not sufficient clues to support a binding mode of complexes to DNA. Viscosity is

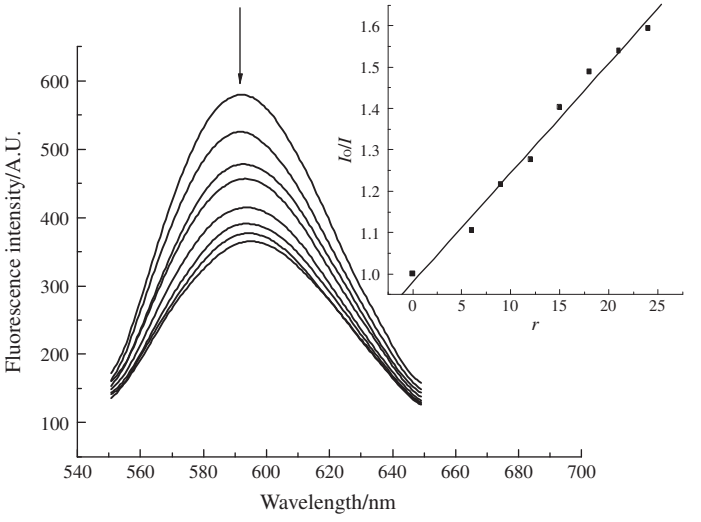

Figure 4. Emission spectra of EB bound to CT-DNA in the presence of $[Cu(HPB)(L\text{-}Arg)(H_2O)](ClO_4)_2$, [EB] $=4.8\times10^{-5}\,M\,L^{-1}$, [DNA] $=5.5\times10^{-5}\,M\,L^{-1}$, [complex]/($10^{-5}$ $M\,L^{-1}$): 0, 1.818, 3.636, 7.272, 10.91, 14.57, 18.18, 21.82, 25.45.

sensitive to the length of DNA and regarded as the least ambiguous and most critical study of the binding mode of metal complexes with CT-DNA in solution and provides strong arguments for intercalative binding in the absence of crystallographic structural data or NMR spectra [43, 44]. To further confirm the binding mode of the present complex with DNA, viscosity measurements were carried out on calf thymus DNA by varying the concentration of the added complex (figure 5).

Figure 5 shows that, upon increasing concentration of the complex, the specific viscosity of CT-DNA increased steadily but is smaller than that bound with EB [40]. This indicates that the complex can intercalate into DNA base pairs [45], consistent with the above spectroscopic results.

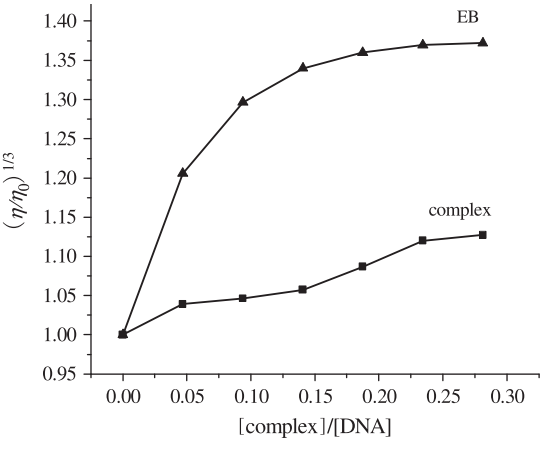

Figure 5. Effects of increasing amounts of $[Cu(HPB)(L\text{-}Arg)(H_2O)](ClO_4)_2$ on the relative viscosity of CT-DNA at 29 ± 0.1 °C. [CT-DNA] $=2\times10^{-4}\,M\,L^{-1}$.

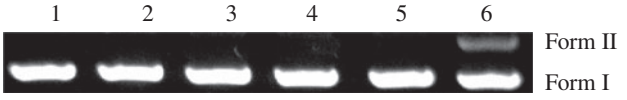

Figure 6. Results of agarose gel electrophoresis of the cleavage of pBR322 DNA by [Cu(HPB)(L-Arg)(H_2O)](ClO_4)$_2$ in 50 mM L^{-1} Tris–HCl/NaCl buffer (pH 7.2) in the presence of reducing agent ascorbate. lane 1: 200 ng pBR322 DNA, lane 2: 200 ng pBR322 DNA + 1.25 mM L^{-1} ascorbate, lane 3: pBR322 DNA + 1.25 mM L^{-1} ascorbate + 25 μM L^{-1} Cu(ClO_4)$_2$, lane 4: 200 ng pBR322DNA + 1.25 mM L^{-1} ascorbate + 25 μM L^{-1} HPB, lane 5: 200 ng pBR322 DNA + 25 μM L^{-1} [Cu(HPB)(L-Arg)(H_2O)](ClO_4)$_2$, lane 6: pBR322 DNA + 1.25 mM L^{-1} ascorbate + 25 μM L^{-1} [Cu(HPB)(L-Arg)(H_2O)](ClO_4)$_2$.

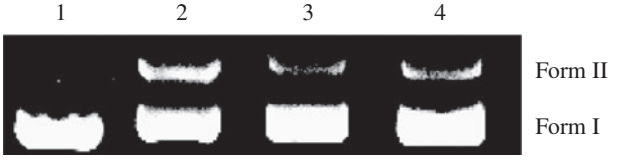

Figure 7. Agarose gel electrophoresis showing the cleavage of pBR322 DNA in the presence of [Cu(HPB)(L-Arg)(H_2O)](ClO_4)$_2$ and ascorbate, or in the presence of [Cu(HPB)(L-Arg)(H_2O)](ClO_4)$_2$, ascorbate, and a potential inhibitor such as DMSO or NaN_3. lane 1: control 200 ng pBR3222 DNA, lane 2: 200 ng pBR3222 DNA + 1.25 mM L^{-1} ascorbate + 25 μM L^{-1} [Cu(HPB)(L-Arg)(H_2O)](ClO_4)$_2$, lane 3: 200 ng pBR3222 DNA + 1.25 mM L^{-1} ascorbate + 25 μM L^{-1} [Cu(HPB)(L-Arg)(H_2O)](ClO_4)$_2$ + 4 μL DMSO, lane 4: 200 ng pBR3222 DNA + 1.25 mM L^{-1} ascorbate + 25 μM L^{-1} [Cu(HPB)(L-Arg)(H_2O)](ClO_4)$_2$ + 100 μM L^{-1} NaN_3.

3.7. *DNA cleavage properties*

The ability of metal complexes to mediate DNA cleavage can be assayed using agarose gel electrophoresis. The cleavage of [Cu(HPB)(L-Arg)(H_2O)](ClO_4)$_2$ to pBR322 DNA in the presence of reducing agent ascorbate is presented in figure 6. In the presence of ascorbate, the complex can induce cleavage of pBR322DNA converted from I to form II (lane 6), but the control experiments using ascorbate, ascorbate + Cu(ClO_4)$_2$, ascorbate + HPB, or the complex alone did not show DNA cleavage (lanes 2–5). The results show that the complex exhibits potent nuclease activity in the presence of the reducing agent.

To explore the DNA cleavage mechanism of the complex, further investigation was performed using DMSO and NaN_3 under the same conditions (figure 7). Hydroxyl radical scavenger (DMSO) and singlet oxygen scavenger (NaN_3) exhibit partial inhibition of the nuclease activity of the complex. This indicates that the DNA cleavage of the complex may involve hydroxyl radical and a singlet oxygen-like copper-oxo species, similar to the 1,10-phenanthroline–copper complex [$(OP)_2Cu^{2+}$] [46].

4. Conclusion

A Cu(II) complex with 2-(2′-pyridyl)benzimidazole and L-arginine has been synthesized and characterized. The complex contains six crystallographically independent complexes **Cu1**, **Cu2**, **Cu3**, **Cu4**, **Cu5**, and **Cu6**, which have distorted square-pyramidal geometries. The complex exhibited higher antibacterial activity than copper(II) perchlorate and HPB, related to coordination of Cu(II) and the ligand. The complex binds to CT-DNA *via* partial intercalation and cleaves plasmid DNA with involvement of hydroxyl radicals and singlet oxygen-like copper-oxo species in the presence of ascorbate.

Acknowledgments

The authors are grateful to the 211 Project Program Foundation of South China Agricultural University (2009B010100001), the Natural Science Foundation of Guangdong (No. 10151064201000016), and the Program of Guangdong Provincial Science & Technology (2009B020312010) for financial support.

References

[1] T. Sugimori, H. Mosuda, N. Ohata, K. Koiwai, A. Odani, O. Yamauchi. *Inorg. Chem.*, **36**, 576 (1997).
[2] H.F. Ma, X.R. Zeng, X.H. Zhou, S. Chen, C.L. Ni. *J. Coord. Chem.*, **61**, 3829 (2008).
[3] M.E. Bravo-Gómez, J.C. García-Ramos, I. Gracia-Mora, L. Ruiz-Azuara. *J. Inorg. Biochem.*, **103**, 299 (2009).
[4] Y.M. Lu, X.Y. Le. *Chin. J. Inorg. Chem.*, **27**, 199 (2011).
[5] X. Li, Z.J. Zhang, C.G. Wang, T. Zhang, K. He, F.H. Deng. *J. Inorg. Biochem.*, **105**, 23 (2011).
[6] Y.M. Lu, Y.H. Chen, Z.B. Ou, S. Chen, C.X. Zhuang, X.Y. Le. *Chin. J. Chem.*, **30**, 303 (2012).
[7] D.A. Horton, G.T. Bourne, M.L. Smythe. *Chem. Rev.*, **103**, 893 (2003).
[8] F. Arjmand, B. Mohani, S. Ahmad. *Eur. J. Med. Chem.*, **40**, 1103 (2005).
[9] K.G. Desai, K.R. Desai. *Bioorg. Med. Chem.*, **14**, 8271 (2006).
[10] O. Sánchez-Guadarrama, H. López-Sandoval, F. Sánchez-Bartéz, I. Gracia-Mora, H. Hoõpfl, N. Barba-Behrens. *J. Inorg. Biochem.*, **103**, 1204 (2009).
[11] N.T. Abdel-Ghani, A.M. Mansour. *Inorg. Chim. Acta*, **373**, 249 (2011).
[12] A.A. El-Sherif, B.J.A. Jeragh. *Spectrochim. Acta, Part A*, **68**, 877 (2007).
[13] M. Devereux, D. O'Shea, A. Kellett, M. McCann, M. Walsh, D. Egan, C. Deegan, K. Kędziora, G. Rosair, H. Müller-Bunz. *J. Inorg. Biochem.*, **101**, 881 (2007).
[14] O. Sánchez-Guadarrama, H. López-Sandoval, F. Sánchez-Bartéz, I. Gracia-Mora, H. Höpfl, N. Barba-Behrens. *J. Inorg. Biochem.*, **103**, 1204 (2009).
[15] Y.M. Lu, Z.B. Ou, H.F. Liu, X.Y. Le. *Chin. J. Inorg. Chem.*, **27**, 704 (2011).
[16] G. Crisponi, V.M. Nurchi, D. Fanni, C. Gerosa, S. Nemolato, G. Faa. *Coord. Chem. Rev.*, **254**, 876 (2010).
[17] P. Živec, F. Perdih, I. Turel, G. Giester, G. Psomas. *J. Inorg. Biochem.*, **117**, 35 (2012).
[18] Y.M. Lu, X.Y. Le. *Acta Crystallogr.*, **E67**, m642 (2011).
[19] S.M. Yue, H.B. Xu, J.F. Ma, Z.M. Su, Y.H. Kan, H.J. Zhang. *Polyhedron*, **25**, 635 (2006).
[20] J. Marmur. *J. Mol. Biol.*, **3**, 208 (1961).
[21] M.E. Reichmann, S.A. Rice, C.A. Thomas, P. Doty. *J. Am. Chem. Soc.*, **76**, 3047 (1954).
[22] Bruker AXS. *SAINT+ (Version, 6.0)*, Bruker AXS, Madison, WI, USA (2001).
[23] G.M. Sheldrick. *SADABS, Program for Empirical Absorption Correction of Area Detector Data*, Gottingen University, Germany (2004).
[24] A.J. Wilson. International Tables for X-ray Crystallography, Vol. C, Kluwer Academic Publishers, Dordrecht (1992), Tables 6.1.1.4 (p. 500) and 4.2.6.8 (p. 219), respectively.
[25] G.M. Sheldrick. *SHELTL-2005, Program for X-ray Crystal Structure Determination*, Gottingen University, Germany (2005).
[26] S. Satyanarayana, J.C. Dabrowiak, J.B. Chaires. *Biochemistry*, **31**, 9319 (1992).
[27] W.J. Gear. *Coord. Chem. Rev.*, **7**, 81 (1971).
[28] Y.M. Lu, Z.B. Ou, W. Hu, X.Y. Le. *Acta Chim. Sinica*, **70**, 973 (2012).
[29] E.K. Efthimiadou, Y. Sanakis, M. Katsarou, C. P. Raptopoulou, A. Karaliota, N. Katsaros, G. Psomas. *J. Inorg. Biochem.*, **100**, 1378 (2006).
[30] M. Zheng, Y.Q. Zheng, B.S. Zhang. *J. Coord. Chem.*, **64**, 3419 (2011).
[31] J.R.J. Sorenson. *Prog. Med. Chem.*, **26**, 437 (1989).
[32] J.R.J. Sorenson. *Handbook of Metal-Ligand Interactions in Biological Fluids*, Vol. 2, 1st Edn, p. 1318, Marcel Decker, New York (1995).
[33] P.S. Subramanian, E. Suresh, P. Dastidar, S. Waghmode, D. Srinivas. *Inorg. Chem.*, **40**, 4291 (2001).
[34] A.A. Abou-Hussein, N.H. Mahmoud, W. Linert. *J. Coord. Chem.*, **64**, 2592 (2011).
[35] S.H. Cui, M. Jiang, Y.T. Li, Z.Y. Wu, X.W. Li. *J. Coord. Chem.*, **64**, 4209 (2011).
[36] S.A. Tysoe, A.D. Baker, T.C. Strekas. *J. Phys. Chem.*, **97**, 1707 (1993).
[37] A. Wolfe, G.H. Shimer, T. Meehan. *Biochemistry*, **26**, 6392 (1987).
[38] J.B. Lepecq, C. Paoletti. *J. Mol. Biol.*, **27**, 87 (1967).
[39] V.G. Vaidyanathan, B.U. Nair. *J. Inorg. Biochem.*, **94**, 121 (2003).
[40] J. Toneatto, R.A. Boero, G. Lorenzatti, A.M. Cabanillas, G.A. Argüello. *J. Inorg. Biochem.*, **104**, 697 (2010).

[41] X.X. Ren, J.Y. Chen, X.Y. Le. *Chin. J. Chem.*, **29**, 1380 (2011).
[42] S.S. Wu, W.B. Yuan, H.Y. Wang, Q. Zhang, M. Liu, K.B. Yu. *J. Inorg. Biochem.*, **102**, 2026 (2008).
[43] S.E. Bryan, D.L. Vizard, D.A. Beary, R.A. LaBiche, K.J. Hardy. *Nucleic Acids Res.*, **9**, 5811 (1981).
[44] H.L. Wu, X.C. Huang, B. Liu, F. Kou, F. Jia, J.K. Yuan, Y. Bai. *J. Coord. Chem.*, **64**, 4383 (2011).
[45] Y. Mei, J.J. Zhou, H. Zhou, Z.Q. Pan. *J. Coord. Chem.*, **65**, 643 (2012).
[46] D.S. Sigman. *Biochemistry*, **29**, 9097 (1990).